Plant Sci. Arc.
Plant Science Archives
An International Journal of Plant Biology

Original Research Article
ISSN 2518-6965
Journal Homepage: www.plantarc.com

Valorization of *Pistia stratiotes* Biomass into Biodegradable Pots for Sustainable Crop Production and Plant Disease Management

Rayapati Saketh, Veeramalla Lingaswamy, Nukathoti Deena Jessica, Shivalingu Ramya, Potharapally Lokesh, and Madhuri K*

Department of Biotechnology, Mahatma Gandhi University, Nalgonda, Telangana, India

Citation: Rayapati Saketh, Veeramalla Lingaswamy, Nukathoti Deena Jessica, Shivalingu Ramya, Potharapally Lokesh, and Madhuri K (2026). Valorization of *Pistia stratiotes* Biomass into Biodegradable Pots for Sustainable Crop Production and Plant Disease Management. *Plant Science Archives.* **DOI: https://doi.org/10.51470/PSA.2026.11.2.121**

Corresponding Author: **Madhuri K** | E-Mail: **(madhuriphd09@yahoo.com)**

Received 23 March 2026 | Revised 21 April 2026 | Accepted 22 May 2026 | Available Online 24 June 2026

ABSTRACT

This study investigated the utilization of invasive Pistia stratiotes (water lettuce) for developing biodegradable nursery pots with antimicrobial and plant growth-promoting properties. The optimized formulation containing P. stratiotes, neem cake, and groundnut shell powder at a 2:1:1 ratio, bound with gelatinised corn starch, produced stable and crack-resistant biopots. The methanolic extract exhibited the highest antibacterial activity against Staphylococcus sp. (2.1 ± 0.15 cm) and E. coli (1.6 ± 0.10 cm), with a functional MIC of 0.625 µL well^{-1}. The aqueous extract inhibited Sclerotium rolfsii and Phytophthora spp. by 56.34 ± 2.81% and 42.22 ± 2.14%, respectively, while the antifungal MIC was 1.25 µg mL^{-1}. GC–MS identified 19 compounds representing 95.70% of the total chromatographic area, with palmitic acid (12.88%), linoleic acid (10.76%), oleic acid (9.94%), β-sitosterol (8.95%), phytol (7.36%), and stigmasterol (6.22%) as major constituents. Tomato germination reached 90.0 ± 2.89% in biopots compared with 70.0 ± 2.89% under chemical treatment and 60.0 ± 2.89% in the control (F = 12.50, p = 0.007). Biopot-grown seedlings recorded a root length of 7.16 ± 0.29 cm, shoot length of 12.67 ± 0.48 cm, fresh biomass of 0.73 ± 0.04 g plant^{-1}, dry biomass of 0.112 ± 0.005 g plant^{-1}, and seed vigour index of 1586.4 ± 41.8. Overall, P. stratiotes-based biopots provide a promising biodegradable alternative to conventional plastic nursery containers while supporting antimicrobial activity and improved tomato seedling establishment.

Keywords: *Pistia stratiotes; water lettuce; biodegradable biopots; antimicrobial activity; antifungal activity; tomato germination; seed vigour index; sustainable agriculture.*

1. Introduction

Modern agriculture faces the dual challenge of increasing food production while reducing dependence on environmentally persistent materials. Plastic nursery containers made from polypropylene, polyethylene, and polystyrene are widely used but persist in agricultural environments and may contribute to microplastic accumulation. Consequently, biodegradable pots produced from renewable lignocellulosic biomass have emerged as sustainable alternatives that can reduce plastic waste and minimize root disturbance during transplantation [1–3]. Biopots manufactured from phytochemically active plant biomass may also provide functions beyond physical seedling support. Plant-derived phenolics, flavonoids, terpenoids, sterols, and other secondary metabolites can exhibit antimicrobial and antifungal activities and may contribute to the suppression of soil-borne pathogens [4–6]. *Pistia stratiotes* L. (water lettuce) is an invasive floating macrophyte that forms dense mats in freshwater systems, obstructing water movement, reducing light and dissolved oxygen, and creating ecological management problems [2,9]. However, its abundant lignocellulosic biomass and reported phenolic, flavonoid, sterol, triterpenoid, alkaloid, tannin, saponin, and glycoside constituents provide opportunities for agricultural valorisation [4,7].

The antimicrobial potential of P. stratiotes is particularly relevant to vegetable nurseries affected by pathogens such as *Fusarium oxysporum*, *Pythium spp.*, *Phytophthora* spp., *Rhizoctonia solani*, and *Ralstonia solanacearum*, which can cause damping-off, root rot, wilt, and seedling mortality [4,5,8]. Although biodegradable containers have been developed from peat, coir, rice straw, paper fibres, and other agricultural residues [1,5,9], the use of P. stratiotes as a multifunctional biopot material remains comparatively underexplored [1,2,6]. GC–MS and ATR–FTIR analyses can further establish relationships between its phytochemical constituents, lignocellulosic structure, and biological functionality [4,10]. Therefore, the present study developed and optimized P. stratiotes-based biodegradable biopots and evaluated their antimicrobial, phytopathogen-suppressive, and plant growth-promoting properties. The investigation incorporated antibacterial and antifungal assays, GC–MS profiling, ATR–FTIR characterization, and evaluation of tomato germination, seedling vigour, biomass, and morphological growth [3,4,6,8–10]. This integrated approach explores the potential of invasive water lettuce biomass as a value-added, biodegradable nursery material for sustainable crop production.

2. Materials and Methods

2.1 Study site and plant material collection

Fresh *Pistia stratiotes* biomass was manually collected from IDL Lake, Kukatpally, Hyderabad, Telangana, India (17°29′N, 78°23′E), where the plant covered approximately 60–70% of the water surface. Leaf length and width were measured from 20 randomly selected rosettes before collection. Whole plants with intact roots were harvested using appropriate protective equipment, drained in open-mesh sacks, and spread on trays to remove excess surface moisture. The biomass was transported to the laboratory on the same day and processed within 2 h of arrival.

2.2 Supplementary raw materials

Locally sourced materials used for biopot preparation included groundnut shell powder, corn starch, deoiled neem and mustard cakes, gum arabic, glycerol, rice husk, sugarcane bagasse, and food-grade sodium benzoate. Groundnut shell served as a structural filler, gelatinised corn starch as the primary binder, neem cake as a filler with potential antifungal functionality, and glycerol as a plasticiser. Sodium benzoate was incorporated as a fungistatic preservative at 0.1% (w/w) of the dry fibre weight.

2.3 Biomass processing

The collected *Pistia stratiotes* plants were dried under sunlight for approximately 48–72 h on raised mesh platforms, and the material was turned twice each day to promote uniform drying. After drying, unwanted debris and other impurities were removed manually. The clean biomass was chopped into small fragments and pulverised in a laboratory grinder using repeated short grinding intervals. The powdered material was then screened through a 250 µm sieve, and any coarse particles were reground until a uniform powder was obtained. The final powder was packed in airtight polypropylene containers and utilised within seven days of preparation. All additional dry ingredients used in the biopot formulations were subjected to the same grinding and sieving procedure to ensure consistency in particle size throughout the experiments.

2.4 Biopot preparation and formulation optimisation

Biopot fabrication was standardised through four sequential trials based on the performance of each preceding formulation. In Batch 1, P. stratiotes, groundnut shell, and neem cake powders were mixed with 5% corn starch solution and shade-dried; however, fungal growth appeared within 24–48 h. Batch 2 used the same composition with direct sun drying, which prevented fungal development but resulted in extensive cracking. In Batch 3, four fibre mixtures containing either 15% corn starch or acacia as binders were evaluated using oven pre-drying followed by sun drying. Although binding strength improved, cracking remained due to moisture and vapour accumulation during heating. For Batch 4, a concentrated gelatinised corn starch binder (30 g/100 mL) was prepared at 75–85°C with continuous stirring and incorporated at an approximate fibre-to-binder dry-weight ratio of 80:20. The moulded pots were then sun-dried for 2–3 days without oven treatment. Two formulations showed satisfactory structural stability without visible cracks: Combination A, consisting of P. stratiotes, neem cake, and groundnut shell powder (2:1:1), and Combination B, containing P. stratiotes and groundnut shell powder (1:1). Sodium benzoate at 0.1% (w/w) was incorporated to minimise fungal development during drying, without observable effects on pot integrity or subsequent seed germination.

2.5 Preparation of extracts for biological evaluation

Crude solvent extracts were prepared from dried, 60-mesh-sieved P. stratiotes powder using four solvents of contrasting polarity methanol, ethyl acetate, n-hexane, and distilled water at a solid-to-solvent ratio of 1:20 (w/v), agitated on a rotary shaker (150 rpm, 48 h, ambient temperature) and filtered through Whatman No. 1 paper. Organic extracts were concentrated under reduced pressure at ≤40°C using a rotary evaporator; the aqueous extract was concentrated by lyophilisation. Extracts were reconstituted at 50 mg/mL for bioassay use and stored at 4°C in amber vials.

2.6 Antibacterial activity by disc diffusion assay

The antibacterial potential of P. stratiotes extracts was assessed against Gram-positive *Bacillus* sp. and *Staphylococcus* sp. and Gram-negative *Escherichia coli* and *Pseudomonas* sp., using authenticated cultures obtained from MTCC, Chandigarh, India. Bacterial suspensions were adjusted to 0.5 McFarland standard (approximately 1.5×10^8 CFU/mL) and uniformly inoculated onto nutrient agar plates. Sterile 6-mm Whatman No. 1 filter-paper discs were impregnated with individual extracts for 15 min and positioned on the inoculated medium. Ampicillin (25 µg/disc) served as the positive control. Following incubation at 37°C for 24–48 h, antibacterial efficacy was determined by measuring the diameter of the inhibition zones in millimetres. All treatments were performed in triplicate (n = 3).

2.7 Determination of antibacterial minimum inhibitory concentration (MIC)

The minimum inhibitory concentration (MIC) of the methanolic P. stratiotes extract was evaluated against E. coli and Staphylococcus sp. using the agar well diffusion technique. Five two-fold serial levels (0.625, 1.25, 2.5, 5.0, and 10.0 µL $well^{-1}$) were introduced into 6-mm wells prepared in inoculated nutrient agar. After incubation at 37°C for 24 h, inhibition zones were measured in millimetres. The MIC was recorded as the lowest tested level that consistently produced a detectable inhibition zone in all three replicates (n = 3).

2.8 Antifungal activity by dual-culture assay

The antifungal efficacy of *P. stratiotes* extracts was examined against *Sclerotium rolfsii* and *Phytophthora* spp. cultured on potato dextrose agar (PDA). A 5-mm mycelial disc obtained from a 96-h-old culture was placed at the centre of each PDA plate, while four extract-impregnated discs were positioned approximately 2 cm from the fungal inoculum. Discs containing only the corresponding solvent were maintained as controls. The plates were incubated at 28–30°C for 48–96 h, and radial mycelial growth was recorded at 48-h intervals. Antifungal activity was expressed as percentage inhibition of radial growth (PIRG), calculated as $[(C - T)/C] \times 100$, where C and T are mean radial growth in control and treated plates. All experiments were conducted in triplicate (n = 3).

2.9 Determination of antifungal minimum inhibitory concentration (MIC)

The antifungal MIC of the methanolic *P. stratiotes* extract was determined against *Sclerotium rolfsii* and *Phytophthora infestans* using PDA containing 0.1% (v/v) DMSO.

Extract concentrations of 1.25, 2.5, 5.0, and 10.0 µg/mL were introduced into 6-mm wells positioned approximately 2 cm from the centrally placed fungal plug. Plates were maintained at 28–30°C for up to 96 h, and inhibition zones were recorded every 24 h. The MIC was considered the lowest concentration that consistently produced a measurable inhibition zone across three independent replicates (n = 3).

2.10 GC-MS analysis

The chemical constituents of the biopot material were characterised by GC–MS following methanolic extraction. Briefly, 5 g of powdered sample was immersed in 50 mL of HPLC-grade methanol (1:10, w/v) and maintained at room temperature for 48 h. The recovered extract was clarified using Whatman No. 1 filter paper followed by a 0.22 µm PTFE syringe membrane and subsequently concentrated under a nitrogen stream at 40°C. Chromatographic separation was performed using an Agilent 7890B GC system interfaced with an Agilent 5977B quadrupole mass-selective detector and equipped with an HP-5MS column (30 m × 0.25 mm; 0.25 µm film thickness). Helium was supplied as the carrier gas at 1 mL min^{-1}. The oven was initially maintained at 60°C for 2 min, increased to 280°C at 10°C min^{-1}, and held at the final temperature for 10 min, giving a total analytical time of 34 min. The injector was maintained at 280°C with a split ratio of 20:1. Mass spectra were recorded under electron ionisation at 70 eV across an *m/z* range of 50–600. Tentative compound identification was based on comparison with the NIST 2020 mass spectral database using a minimum similarity threshold of 80%, with additional support from retention indices determined using a C8–C30 *n*-alkane standard series. The proportional abundance of each detected constituent was calculated from its normalised chromatographic peak area.

2.11 FTIR Spectroscopic analysis

ATR–FTIR analysis of the dried and finely powdered biopot material was performed at the Central Instrumentation Facilities, Osmania University, Hyderabad. Spectra were acquired using a PerkinElmer Spectrum 100 spectrometer equipped with a universal ATR accessory over the range of 4000–400 cm^{-1}, at a resolution of 4 cm^{-1} with 16 accumulated scans per sample. A fresh background spectrum was recorded before each measurement. The resulting absorbance spectra were baseline-corrected, and the major absorption bands were interpreted using established FTIR functional-group assignments to identify the principal chemical components present in the biopot matrix.

2.12 Seed germination and pot experiments

The influence of *P. stratiotes* on tomato (*Solanum lycopersicum*) germination was initially examined using the paper-towel method following ISTA Rules (2022). Seeds were pre-soaked for 12 h and subjected to three treatments: distilled water (control), a commercial plant-growth promoter (chemical treatment), and *P. stratiotes* aqueous extract (1:10, w/v).

A subsequent pot experiment compared seedling emergence in autoclaved and non-autoclaved soil using the optimised Batch-4 biopots containing pre-soaked tomato seeds, while soil without biopots served as the control. Emergence was recorded at 7, 14, and 21 days. Plant-growth performance was further assessed for 30 days by comparing foliar application of *P. stratiotes* aqueous extract (1:10, w/v) with water and commercial growth-promoter treatments. At the end of the experiment, plant height, number of leaves, leaf dimensions, primary root length, and fresh aerial biomass were recorded.

2.13 Statistical analysis

Experimental data were analysed using IBM SPSS Statistics version 26. Percentage germination values were subjected to arcsine square-root transformation before parametric testing, and data distribution was examined using the Shapiro–Wilk test. Normally distributed datasets were evaluated by one-way analysis of variance (ANOVA), followed by Tukey's honestly significant difference (HSD) test for multiple comparisons. Differences were considered statistically significant at $p < 0.05$. Inhibition-zone data involving two groups were compared using independent-samples *t*-tests, whereas datasets containing more than two groups were analysed by one-way ANOVA followed by Tukey's HSD test. Graphical presentation of the results was generated using GraphPad Prism version 9.0 and Microsoft Excel 2019.

3. Results

3.1 Optimisation of biopot formulation and fabrication

The fabrication process showed clear improvement across the four successive optimisation batches, with each modification addressing limitations identified during the preceding trial (Table 1; Figs. 1–3). The first batch, prepared from *P. stratiotes* powder, groundnut shell powder, and neem cake powder using 5% corn starch solution, exhibited extensive fungal development within 24–48 h of shade drying. The high moisture retention and comparatively slow drying of the fibre–starch matrix appeared unsuitable for maintaining the pots free from visible microbial contamination. Consequently, these pots were discarded and the drying procedure was modified in the subsequent batch.

Figure 1: Collection, harvesting, and processing of Pistia stratiotes from urban freshwater ecosystems, Hyderabad, India. (A) Dense P. stratiotes mat on an urban lake surface. (B) Field survey and collection. (C) Harvested biomass prepared for laboratory processing

Table 1: Summary of Pistia stratiotes biopot fabrication batches — formulations, binders, drying methods, and outcomes

Batch	Formulation	Binder	Drying	Outcome
1st	Pistia powder + groundnut shell powder + neem cake powder	5% corn starch solution	Shade (2–3 d)	Pervasive fungal contamination within 24–48 h; discarded
2nd	Same as 1st (unchanged)	5% corn starch solution	Direct sun (8 d)	No contamination; severe structural cracking
3rd	4 fibre combinations; acacia or corn starch binder	15% acacia / corn starch	Oven + solar	Improved cohesion; cracking persists (steam-driven)
4th	Combination A (2:1:1) / Combination B (1:1)	Thick gelatinised corn starch gel (80:20)	Direct sun (2–3 d)	Crack-free, structurally sound; 0.1% sodium benzoate-controlled contamination

Figure 2: Development and drying of eco-friendly water lettuce-based biopots (Batch 2/3 trials)

Figure 3: Preparation and final production of Pistia stratiotes-based biopots (optimised Batch 4)

In Batch 2, the original formulation and binder concentration were maintained, but shade drying was replaced with direct sunlight. Solar drying effectively prevented visible fungal growth; however, substantial surface and structural cracking occurred during moisture loss, indicating poor dimensional stability caused by rapid and uneven drying. In Batch 3, four fibre combinations were tested with either acacia or corn starch at an increased binder concentration of 15%. Although oven pre-drying followed by solar drying improved particle cohesion, cracking persisted, suggesting that rapid internal moisture loss during oven treatment adversely affected structural integrity.

Batch 4 produced the most satisfactory biopots following modification of both binder preparation and drying conditions. A fully gelatinised corn starch gel was incorporated at an approximately 80:20 fibre-to-binder dry-weight ratio, oven treatment was eliminated, and the moulded pots were sun-dried for 2–3 days. Both Combination A (P. stratiotes:neem cake:groundnut shell powder, 2:1:1) and Combination B (P. stratiotes:groundnut shell powder, 1:1) produced intact, crack-free pots with satisfactory cohesion and handling stability. Addition of 0.1% (w/w) sodium benzoate prevented visible fungal contamination without apparent adverse effects on pot structure or seed germination. Overall, Batch 4 provided the optimal balance of structural integrity, microbial stability, and suitability for subsequent plant-growth experiments and was therefore selected for further evaluation.

3.2 Antibacterial Activity of *Pistia stratiotes* Extracts

Antibacterial screening showed that all four P. stratiotes extracts inhibited the tested bacteria, with activity varying according to solvent and bacterial species (Table 2; Figs. 4–5). The methanolic extract showed the highest activity, producing inhibition zones of 2.1 ± 0.15 cm against Staphylococcus sp., 1.8 ± 0.12 cm against Bacillus sp., 1.6 ± 0.10 cm against E. coli, and 1.4 ± 0.09 cm against Pseudomonas sp. Ethyl acetate showed moderate activity (1.0 ± 0.07–1.7 ± 0.10 cm), while the aqueous extract produced inhibition zones ranging from 0.9 ± 0.06 to 1.5 ± 0.09 cm. The n-hexane extract showed the lowest antibacterial activity, with inhibition zones ranging from 0.8 ± 0.05 to 1.2 ± 0.08 cm. Overall, antibacterial effectiveness followed the order methanol > ethyl acetate > aqueous > n-hexane. Staphylococcus sp. was the most susceptible organism, whereas Pseudomonas sp. was consistently the least susceptible. The ampicillin control produced a 2.8 ± 0.10 cm inhibition zone against all tested organisms. These findings demonstrate that P. stratiotes possess measurable antibacterial activity, with the methanolic extract exhibiting the strongest inhibitory potential among the tested fractions.

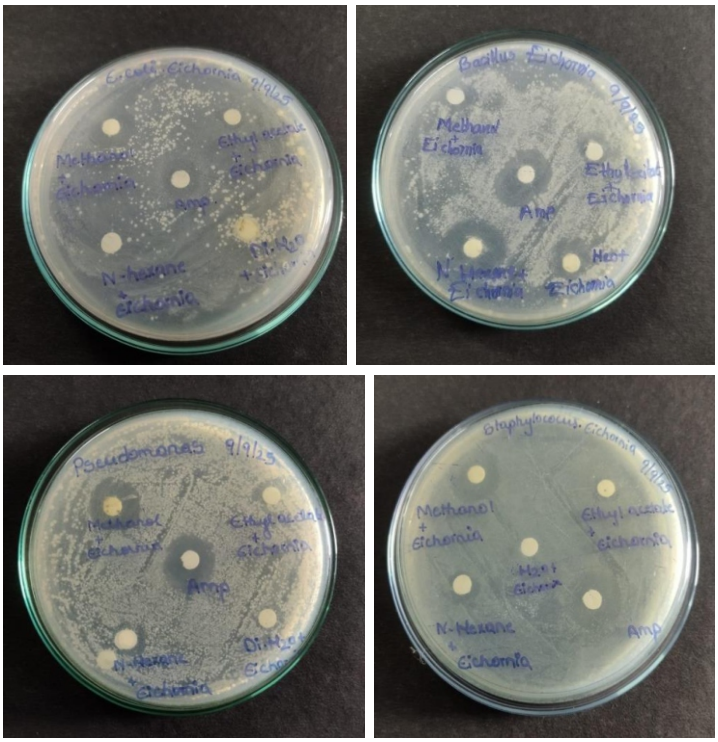

Figure 4: Antibacterial activity of different solvent extracts of Pistia stratiotes against selected bacterial pathogens (agar well/disc diffusion assay)

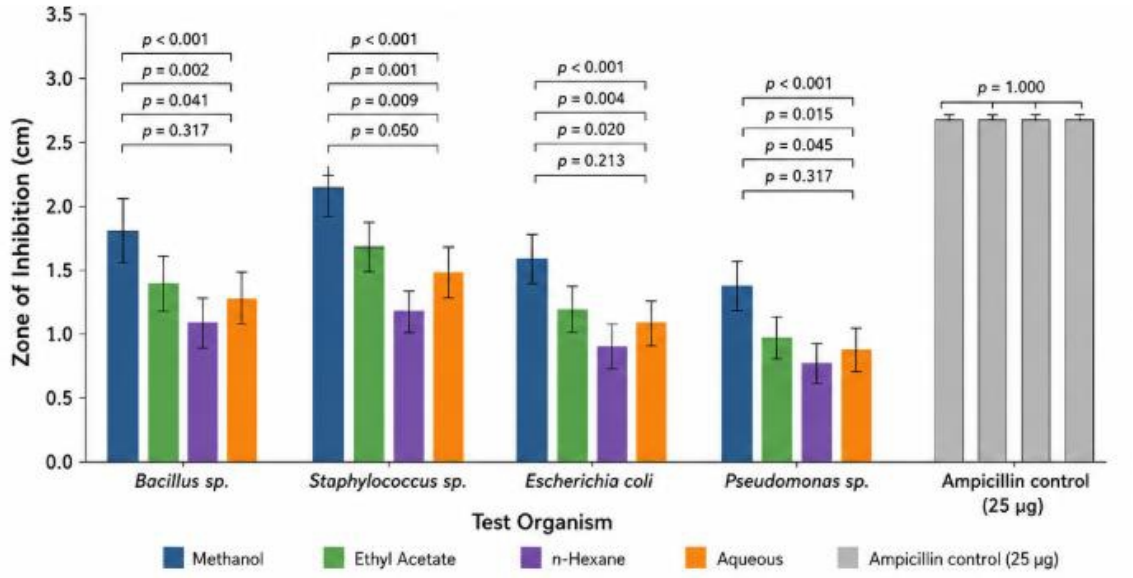

Figure 5: Comparative antibacterial activity of different solvent extracts of Pistia stratiotes against selected bacterial pathogens.

Table 2: Zones of inhibition (cm ± SD, n = 3) produced by four solvent extracts of Pistia stratiotes against test bacteria; ampicillin (25 µg) as positive control

Test organism	Methanol	Ethyl acetate	n-Hexane	Aqueous	Ampicillin (25 µg)
Bacillus sp.	1.8 ± 0.12	1.4 ± 0.09	1.1 ± 0.07	1.3 ± 0.11	2.8 ± 0.10
Staphylococcus sp.	2.1 ± 0.15	1.7 ± 0.10	1.2 ± 0.08	1.5 ± 0.09	2.8 ± 0.10
Escherichia coli	1.6 ± 0.10	1.2 ± 0.08	0.9 ± 0.06	1.1 ± 0.07	2.8 ± 0.10
Pseudomonas sp.	1.4 ± 0.09	1.0 ± 0.07	0.8 ± 0.05	0.9 ± 0.06	2.8 ± 0.10

3.3 Minimum inhibitory concentration (MIC) — Antibacterial activity

Both *Escherichia coli* and *Staphylococcus* sp. exhibited a clear volume-dependent antibacterial response, with inhibition generally increasing as the applied volume increased from 0.625 to 10.0 µL/well. At the lowest volume of 0.625 µL/well, inhibition zones of 0.4 cm and 0.6 cm were recorded for *E. coli* and *Staphylococcus* sp., respectively. Increasing the volume to 1.25 µL/well increased the zones to 0.6 cm for *E. coli* and 0.7 cm for *Staphylococcus* sp. At 2.5 µL/well, the inhibition zones reached 0.9 cm and 0.8 cm, respectively, while both organisms showed an equal inhibition zone of 1.0 cm at 5.0 µL/well. The highest antibacterial activity was observed at 10.0 µL/well, producing inhibition zones of 1.1 cm against *E. coli* and 1.4 cm against *Staphylococcus* sp. Overall, *Staphylococcus* sp. showed greater susceptibility at most tested volumes, although *E. coli* produced slightly greater inhibition at 2.5 µL/well. Statistical analysis confirmed significant effects of bacterial species ($F(1,20) = 8.91$, $p = 0.0070$) and treatment volume ($F(4,20) = 45.68$, $p < 0.0001$). The species × volume interaction was also significant ($F(4,20) = 2.78$, $p = 0.0493$), indicating differences in the response pattern of the two organisms across treatment levels. Since detectable inhibition was observed at 0.625 µL/well for both bacteria, this concentration was considered the lowest tested effective volume under the experimental conditions (Fig. 6).

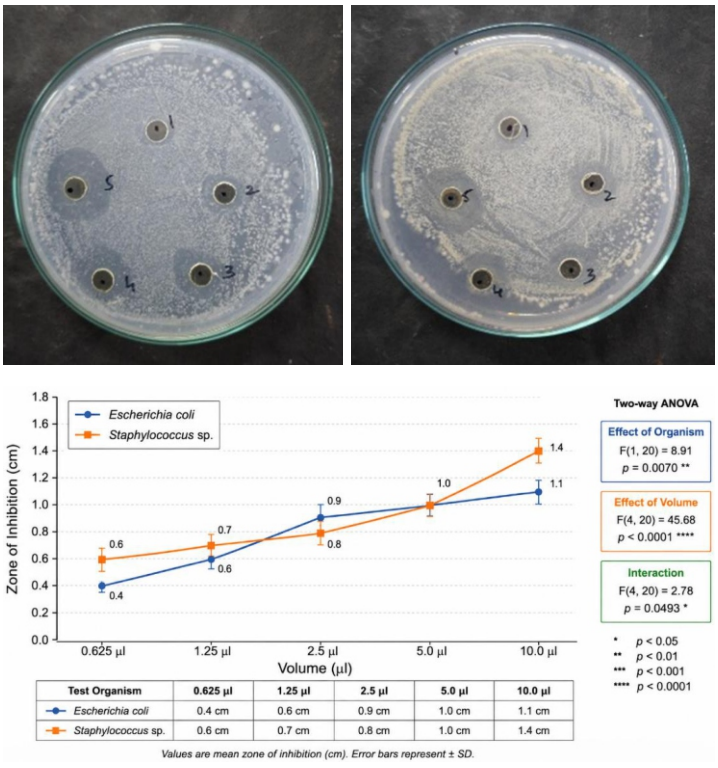

Figure 6: Minimum inhibitory concentration (MIC) assay showing zones of inhibition (cm) produced by P. stratiotes methanolic extract

3.4 Antifungal activity — Dual culture assay

The antifungal activity of four P. stratiotes solvent extracts was evaluated against *Sclerotium rolfsii* and *Phytophthora* spp. using the dual culture assay on PDA. Radial growth inhibition was measured after 96 h and expressed as mean percentage inhibition ± standard deviation from three replicates (Table 3; Fig. 7). Clear differences were observed among the extracts, with antifungal effectiveness following the order aqueous > methanol > ethyl acetate > n-hexane. Across all treatments, *S. rolfsii* was more susceptible than Phytophthora spp. The aqueous extract showed the strongest antifungal activity, producing 56.34 ± 2.81% inhibition against *S. rolfsii* and 42.22 ± 2.14% against *Phytophthora* spp. The methanolic extract ranked second, with inhibition values of 48.70 ± 2.30% and 37.90 ± 1.95%, respectively. These results indicate that the more polar extracts contained a greater proportion of constituents capable of restricting pathogen growth under the tested conditions.

Moderate antifungal activity was observed with the ethyl acetate extract, which inhibited *S. rolfsii* by 39.45 ± 1.98% and *Phytophthora* spp. by 31.18 ± 1.62%. In comparison, the n-hexane fraction showed the weakest response, with inhibition values of 28.33 ± 1.55% against *S. rolfsii* and 22.76 ± 1.30% against *Phytophthora* spp. Overall, the results demonstrate substantial variation in antifungal activity according to extraction solvent, with the aqueous fraction providing the greatest suppression of both tested pathogens.

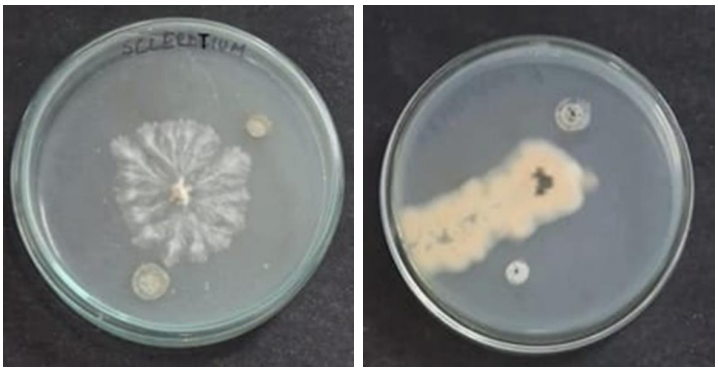

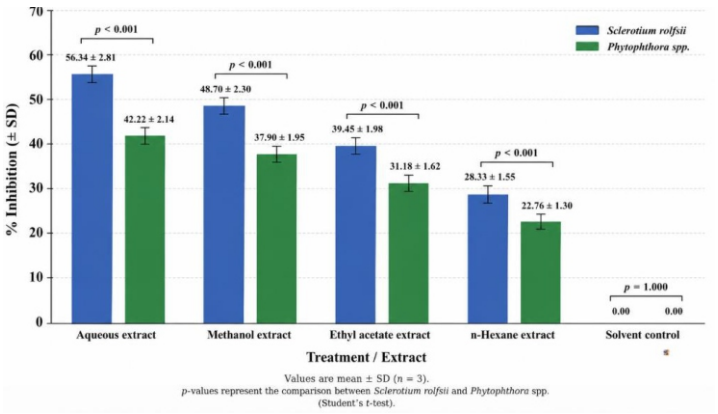

Figure 7: Antifungal activity of different solvent extracts against Sclerotium rolfsii and Phytophthora spp

Table 3: Percentage inhibition of radial growth of Sclerotium rolfsii and Phytophthora spp. by four solvent extracts dual culture assay on PDA at 96 h

Treatment / extract	*Sclerotium rolfsii* % inhibition	*Phytophthora* spp. % inhibition
Aqueous extract	56.34 ± 2.81	42.22 ± 2.14
Methanol extract	48.70 ± 2.30	37.90 ± 1.95
Ethyl acetate extract	39.45 ± 1.98	31.18 ± 1.62
n-Hexane extract	28.33 ± 1.55	22.76 ± 1.30
Solvent control	0.00	0.00

A clear pathogen-specific response was observed across all solvent extracts, with *S. rolfsii* consistently showing greater susceptibility than *Phytophthora* spp. The greatest difference occurred with the aqueous extract, which produced 56.34% inhibition of *S. rolfsii* compared with 42.22% inhibition of *Phytophthora* spp. A similar response pattern was maintained with methanol, ethyl acetate, and *n*-hexane extracts, confirming comparatively lower sensitivity of *Phytophthora* spp. under the same experimental conditions. The solvent control showed 0.00% inhibition against both pathogens, confirming that the observed growth suppression was attributable to constituents present in the *P. stratiotes* extracts rather than to the solvent itself. Overall, the aqueous extract was the most effective antifungal fraction, particularly against *S. rolfsii*. The gradual decline in activity from aqueous to methanol, ethyl acetate, and *n*-hexane fractions suggests that the principal antifungal constituents were predominantly associated with the polar and moderately polar fractions.

3.5 Minimum inhibitory concentration — Antifungal

The concentration-dependent antifungal activity of the *Pistia stratiotes* methanolic extract was evaluated against *Sclerotium rolfsii* and *Phytophthora* spp. at 1.25, 2.5, 5.0, and 10.0 µg/mL (Table 4). Both pathogens were inhibited even at the lowest concentration, although their responses differed with increasing extract concentration. For *S. rolfsii*, inhibition increased steadily from 28.1% at 1.25 µg/mL to 31.25% at 2.5 µg/mL and 35.6% at 5.0 µg/mL, reaching a maximum of 41.2% at 10.0 µg/mL. This represented an overall increase of 13.1 percentage points and demonstrated a consistent concentration-dependent response. *Phytophthora* spp. showed greater sensitivity at the lower and intermediate concentrations, with inhibition increasing from 36.6% at 1.25 µg/mL to 41.2% at 2.5 µg/mL and reaching a maximum of 45.6% at 5.0 µg/mL. At 10.0 µg/mL, inhibition slightly decreased to 42.2%, indicating a possible response plateau or normal experimental variation rather than a substantial loss of activity. At 1.25, 2.5, and 5.0 µg/mL, *Phytophthora* spp. consistently showed greater inhibition than *S. rolfsii*. However, at 10.0 µg/mL, the responses became comparable, with 42.2% inhibition for *Phytophthora* spp. and 41.2% for *S. rolfsii*. Overall, the methanolic extract demonstrated effective concentration-responsive antifungal activity, with *Phytophthora* spp. responding more strongly at lower concentrations and *S. rolfsii* showing a continuous increase in inhibition across the tested range (Fig. 8).

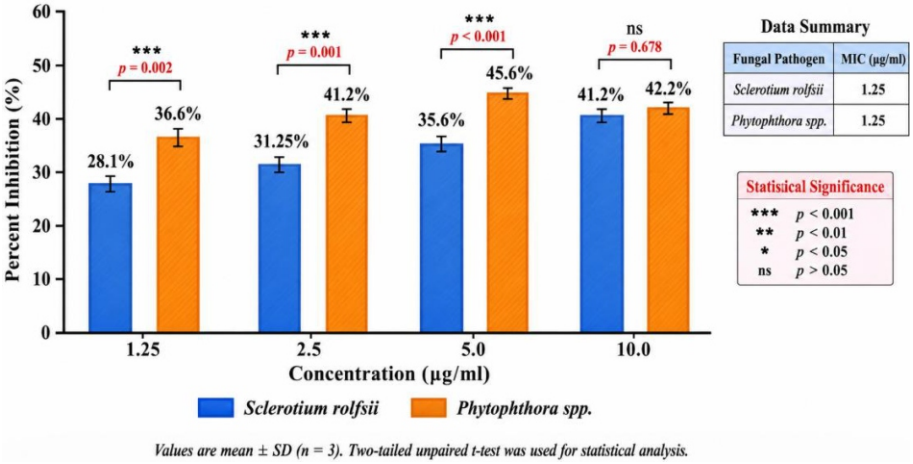

Figure 8. Concentration-dependent antifungal activity of P. stratiotes methanolic extract against Sclerotium rolfsii and Phytophthora spp.

Table 4: Percentage inhibition of mycelial growth by P. stratiotes methanolic extract at four concentrations — antifungal MIC determination on PDA

Fungal pathogen	1.25 µg/mL	2.5 µg/mL	5.0 µg/mL	10.0 µg/mL	MIC (µg/mL)
Sclerotium rolfsii	28.1%	31.25%	35.6%	41.2%	1.25
Phytophthora spp.	36.6%	41.2%	45.6%	42.2%	1.25

Statistical analysis confirmed significant differences between *S. rolfsii* and *Phytophthora* spp. at 1.25 µg/mL (p = 0.002), 2.5 µg/mL (p = 0.001), and 5.0 µg/mL (p < 0.001). However, at 10.0 µg/mL, the difference was non-significant (p = 0.678), corresponding to the similar inhibition values of 41.2% for *S. rolfsii* and 42.2% for *Phytophthora* spp. This indicates that pathogen-specific sensitivity was more evident at lower and intermediate concentrations and decreased at the highest concentration.

3.6 GC-MS analysis of biopot biomass

GC–MS profiling of the *Pistia stratiotes* biopot biomass methanolic extract revealed a diverse mixture of fatty acids, phenolics, terpenoids, phytosterols, fatty aldehydes, hydrocarbons, fatty alcohols, and carbohydrate-derived compounds. Based on the NIST 2020 spectral library with a ≥80% match threshold, 19 compounds were putatively identified between 7.84 and 30.05 min (Table 5; Fig. 9), representing approximately 99.70% of the total chromatographic area. Lipid-associated compounds formed the dominant fraction, with hexadecanal, palmitic acid, linoleic acid, oleic acid, and stearic acid collectively contributing 40.84%. Palmitic acid was the most abundant compound (12.88%; RT 17.62 min), followed by linoleic acid (10.76%; 18.95 min), oleic acid (9.94%; 19.08 min), stearic acid (5.21%), and hexadecanal (2.05%). Phytosterols and terpenoid-related constituents also represented a major fraction of the extract.

B Sitosterol accounted for 8.95% of the chromatographic area, followed by phytol (7.36%), stigmasterol (6.22%), friedelin (5.25%), squalene (4.87%), lupeol (3.71%), and campesterol (3.02%), together contributing approximately 39.38%. Phenolic constituents included 2-methoxy-4-vinylphenol (3.42%; RT 7.84 min), vanillin (2.11%; 9.12 min), and 4-hydroxybenzoic acid (1.74%; 10.36 min), collectively accounting for 7.27%. Overall, the GC–MS profile demonstrates that the biopot biomass retained substantial lipid, phytosterol, terpenoid, and phenolic constituents, which may collectively contribute to the antimicrobial and other biological activities observed for the *P. stratiotes* extract.

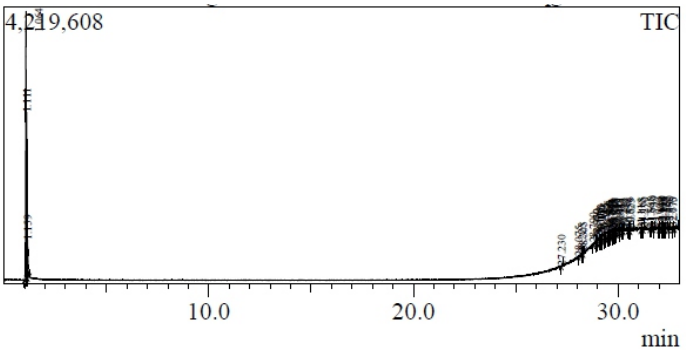

Figure 9: GC-MS chromatogram detail showing major compound peaks identified in Pistia stratiotes biopot extract

Table 5: GC-MS putative compound identification in Pistia stratiotes biopot biomass methanol extract (NIST 2020 match ≥80%)

Peak	RT (min)	Compound	MW	Area (%)	Reported role
1	7.84	2-Methoxy-4-vinylphenol	150.17	3.42	Phenolic — antimicrobial, antioxidant
2	9.12	Vanillin	152.15	2.11	Aldehyde phenolic — antimicrobial
3	10.36	4-Hydroxybenzoic acid	138.12	1.74	Phenolic acid — antifungal
4	12.08	Levoglucosan	162.14	4.63	Polysaccharide degradation marker
5	16.44	Hexadecanal	240.42	2.05	Fatty aldehyde — antimicrobial
6	17.62	Palmitic acid	256.42	12.88	Saturated FA — membrane-disruptive
7	18.95	Linoleic acid	280.45	10.76	PUFA — antifungal, anti-inflammatory
8	19.08	Oleic acid	282.47	9.94	MUFA — antimicrobial synergist
9	19.66	Stearic acid	284.48	5.21	Saturated FA — hydrophobic barrier
10	20.42	Phytol	296.54	7.36	Diterpene alcohol — antimicrobial
11	22.10	1-Docosene	308.59	2.26	Alkene — moisture barrier
12	23.48	1-Tetracosanol	354.66	2.18	Fatty alcohol — surface protection
13	24.92	Tocopherol (α)	430.71	3.14	Vitamin E — antioxidant
14	26.18	Squalene	410.73	4.87	Triterpene — antifungal
15	27.06	Stigmasterol	412.69	6.22	Phytosterol — antifungal
16	27.54	β-Sitosterol	414.71	8.95	Phytosterol — antimicrobial
17	28.12	Campesterol	400.68	3.02	Phytosterol — structural
18	29.30	Friedelin	426.72	5.25	Triterpenoid — antimicrobial
19	30.05	Lupeol	426.72	3.71	Pentacyclic triterpene — antifungal

The chromatographic profile also revealed several additional constituents from different chemical classes. Levoglucosan, detected at 12.08 min, contributed 4.63% of the total peak area, indicating the presence of carbohydrate-derived biomass components. Long-chain compounds included 1-docosene (2.26%) and 1-tetracosanol (2.18%), while α-tocopherol was detected at 24.92 min with an area contribution of 3.14%, confirming the retention of naturally occurring antioxidant constituents in the biopot biomass.

3.7 FTIR Spectroscopic Analysis

ATR–FTIR analysis of the *Pistia stratiotes* biopot biomass revealed thirteen distinct absorption bands between 3361 and 602 cm^{-1} (Table 6; Fig. 10), demonstrating the chemically heterogeneous nature of the material. The detected bands were mainly associated with lignocellulosic carbohydrates, lignin, proteins, lipids, fatty acids, phenolic compounds, and other oxygen-containing functional groups, confirming the characteristic composition of a plant-derived biomass matrix.

The broad, intense band at 3361 cm^{-1} was assigned primarily to O–H stretching vibrations of cellulose, hemicellulose, bound water, and phenolic hydroxyl groups. Its strong intensity indicates an abundance of hydroxyl-containing components capable of hydrogen bonding and contributing to moisture interaction within the biopot matrix. The band at 3219 cm^{-1} was attributed to overlapping O–H and N–H stretching vibrations associated with phenolic and proteinaceous constituents. These spectral features confirm that the processed *P. stratiotes* biomass retained important oxygen- and nitrogen-containing functional groups after biopot fabrication.

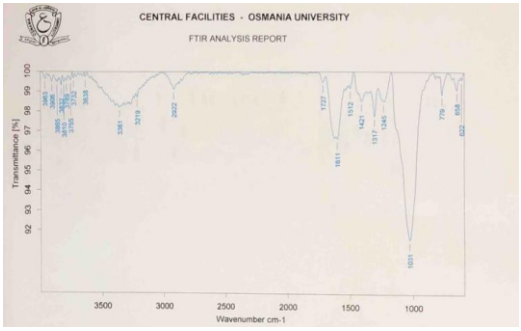

Figure 10: FTIR spectrum of Pistia stratiotes biopot biomass

Table 6: ATR-FTIR spectral peak assignments for Pistia stratiotes biopot biomass

Peak (cm^{-1})	Functional group	Probable biomolecules	Significance
3361	O–H stretching (broad)	Cellulose, hemicellulose, phenols	Water retention; biodegradability indicator
3219	O–H / N–H stretching	Phenolics, proteins	Antioxidant phenol; protein N–H
2922	C–H stretching (asym.)	Lipids, fatty acids, waxes	Hydrophobic barrier; corroborates GC-MS FA dominance
1727	C=O stretching	Carboxylic acids, hemicellulose esters	Ester-linked polysaccharide; phenolic acids
1611	C=C / Amide I	Lignin aromatic ring, proteins	Structural lignin; disease suppression
1512	Aromatic C=C	Lignin, polyphenols	Diagnostic lignin band; antifungal phenolics
1421	CH_2 scissoring	Cellulose, lignin	Crystalline cellulose; mechanical strength
1317	C–N / O–H bending	Proteins, phenols, amides	Bioactive N-containing fractions
1245	C–O–C / aryl C–O	Hemicellulose, lignin esters	Ether-linked polysaccharide scaffold
1031	C–O–C glycosidic	Cellulose, hemicellulose	Dominant structural peak
779	Aromatic C–H o.o.p.	Lignin compounds	Structural + antifungal role
685	Aromatic o.o.p. bending	Phenolic derivatives	Phenolic bioactivity
602	C–Cl / aromatic C–H	Lignin residues	Structural complexity

The absorption band at 2922 cm^{-1} was assigned to aliphatic C–H stretching of CH_2 and CH_3 groups associated with lipids, fatty acids, waxes, and long-chain hydrocarbons. This observation agrees with the GC–MS detection of major fatty acids, including palmitic, linoleic, oleic, and stearic acids, and confirms the presence of lipid-associated constituents in the biopot biomass. The carbonyl band at 1727 cm^{-1} corresponded to C=O stretching of carboxylic acids, ester groups, and oxygenated compounds, indicating the retention of fatty-acid- and hemicellulose-associated functionalities after processing. The bands at 1611 and 1512 cm^{-1} were attributed to aromatic C=C and skeletal vibrations associated mainly with lignin and polyphenolic structures. Their presence indicates that aromatic lignin-derived components remained within the fabricated material. The absorption at 1421 cm^{-1}, corresponding mainly to CH_2 bending, further supported the presence of cellulose and lignin, while the 1317 cm^{-1} band was associated with C–N stretching and O–H bending from proteinaceous and phenolic components.

In the fingerprint region, the 1245 cm^{-1} band was assigned to C–O–C and aryl C–O stretching associated with hemicellulose and lignin. The prominent band at 1031 cm^{-1} represented C–O and C–O–C stretching of glycosidic linkages in cellulose and hemicellulose, confirming polysaccharides as major structural components of the biopot matrix. Bands at 779 and 685 cm^{-1} were associated with aromatic C–H bending of lignin and phenolic structures, whereas the 602 cm^{-1} signal reflected complex vibrations within the low-frequency fingerprint region. Overall, the ATR–FTIR profile showed good agreement with the GC–MS results. The 2922 cm^{-1} band supported the abundance of fatty-acid and lipid-derived compounds, while the bands at 1611, 1512, 779, and 685 cm^{-1} confirmed aromatic lignin- and phenolic-associated structures. Similarly, the 1727 cm^{-1} carbonyl band supported the presence of carboxylic and ester-containing constituents.

Together, these findings confirm that the *P. stratiotes* biopot retained both lignocellulosic structural components and chemically diverse secondary metabolites after fabrication.

3.8 Seed germination and seedling growth of Tomato

Tomato seed germination varied significantly among the treatments, with water lettuce-based biopots producing the highest germination of 90.0 ± 2.89% (9 of 10 seeds), compared with 70.0 ± 2.89% under chemical treatment and 60.0 ± 2.89% in the untreated control (Table 7; Fig. 11). One-way ANOVA confirmed significant treatment differences ($F = 12.50$, $p = 0.007$), with Tukey's HSD further separating the treatment means. The biopot treatment improved germination by approximately 33.3% compared with the control, indicating more favourable conditions for early seed establishment. A similar improvement was observed in seedling development. Biopot-grown seedlings recorded the greatest root length (7.16 ± 0.29 cm) and shoot length (12.67 ± 0.48 cm), followed by the chemical treatment with 5.94 ± 0.25 cm and 10.24 ± 0.41 cm, respectively. Control seedlings showed the lowest root (4.82 ± 0.21 cm) and shoot (8.15 ± 0.32 cm) lengths. Treatment effects were significant for both root length ($F = 18.74$, $p = 0.003$) and shoot length ($F = 26.51$, $p = 0.001$). Compared with the control, biopots increased root and shoot length by approximately 48.5% and 55.5%, respectively, demonstrating improved early vegetative growth.

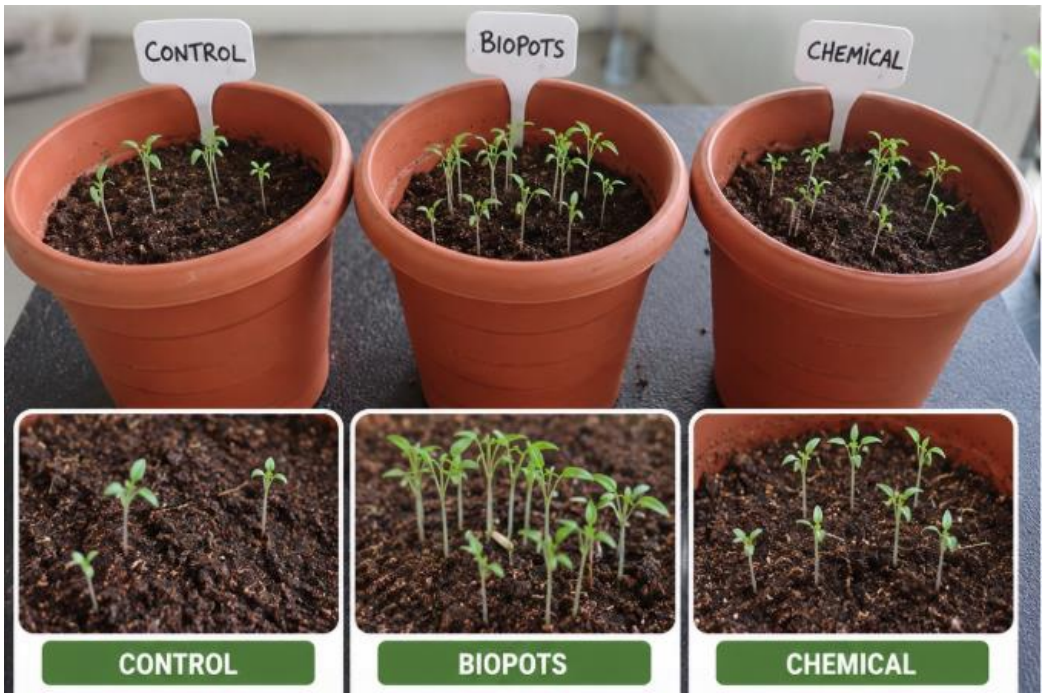

Figure 11: Effect of water lettuce-based biopots on tomato seed germination compared with chemical treatment and control

Table 7: Effect of treatments on tomato seed germination

Treatment	Seeds sown (n)	Seeds germinated	Germination (%) mean ± SE	F-value	p-value
Control	10	6	60.0 ± 2.89[a]	12.50	0.007
Chemical	10	7	70.0 ± 2.89[b]	12.50	0.007
Biopots	10	9	90.0 ± 2.89[c]	12.50	0.007

Biomass accumulation showed a clear treatment-dependent response. Fresh weight was highest in biopot-grown seedlings (0.73 ± 0.04 g plant^{-1}), followed by the chemical treatment (0.56 ± 0.03 g plant^{-1}) and control (0.42 ± 0.02 g plant^{-1}). Similarly, dry weight reached 0.112 ± 0.005 g plant^{-1} in biopots, compared with 0.084 ± 0.004 g plant^{-1} under chemical treatment and 0.061 ± 0.003 g plant^{-1} in the control. Significant treatment effects were observed for both fresh weight ($F = 21.37$, $p = 0.002$) and dry weight ($F = 17.92$, $p = 0.004$). Relative to the control, biopots increased fresh and dry biomass by approximately 73.8% and 83.6%, respectively (Table. 8).

Table 8: Effect of treatments on tomato seedling growth and vigour

Treatment	Root length (cm)	Shoot length (cm)	Fresh weight (g/plant)	Dry weight (g/plant)	Seed vigour index
Control	4.82 ± 0.21[a]	8.15 ± 0.32[a]	0.42 ± 0.02[a]	0.061 ± 0.003[a]	778.2 ± 25.6[a]
Chemical	5.94 ± 0.25[b]	10.24 ± 0.41[b]	0.56 ± 0.03[b]	0.084 ± 0.004[b]	1132.6 ± 32.4[b]
Biopots	7.16 ± 0.29[c]	12.67 ± 0.48[c]	0.73 ± 0.04[c]	0.112 ± 0.005[c]	1586.4 ± 41.8[c]
F-value	18.74	26.51	21.37	17.92	42.68
p-value	0.003	0.001	0.002	0.004	<0.001

Seed vigour showed an even stronger response, reaching 1586.4 ± 41.8 in the biopot treatment compared with 1132.6 ± 32.4 under chemical treatment and 778.2 ± 25.6 in the control. The differences were highly significant ($F = 42.68$, $p < 0.001$), with biopots producing an approximately 103.9% increase in vigour over the control. Overall, water lettuce-based biopots consistently enhanced tomato seedling establishment, biomass accumulation, and vigour, demonstrating their potential as a biodegradable and supportive nursery cultivation system.

3.9 Pot growth studies — Tomato morphology

The morphological characteristics of tomato seedlings varied significantly among the control, chemical, and water lettuce-based biopot treatments (Table 9; Fig. 12). Biopot-grown seedlings showed the greatest plant height (12.67 ± 0.48 cm), compared with the chemical treatment (10.24 ± 0.41 cm) and control (8.15 ± 0.32 cm), representing a 55.5% increase over the control.

Leaf number followed the same pattern, reaching 8.33 ± 0.33 leaves in biopots, 6.33 ± 0.33 under chemical treatment, and 4.67 ± 0.33 in the control. This corresponded to a 78.4% increase over the control, the highest proportional improvement among the measured morphological traits. Leaf dimensions were also enhanced by the biopot treatment. Leaf length increased to 5.36 ± 0.21 cm in biopot-grown seedlings compared with 4.18 ± 0.17 cm under chemical treatment and 3.24 ± 0.14 cm in the control, equivalent to a 65.4% improvement. Similarly, leaf width reached 2.78 ± 0.11 cm in biopots, compared with 2.14 ± 0.09 cm and 1.62 ± 0.08 cm in the chemical and control treatments, respectively, representing a 71.6% increase over the control. These results demonstrate that water lettuce-based biopots substantially promoted tomato seedling growth, leaf formation, and leaf expansion.

Figure 12: Effect of water lettuce-based biopots on tomato seedling emergence and disease suppression

Table 9: Effect of treatments on morphological parameters of tomato seedlings, and percentage increase of biopots over control

Treatment	Plant height (cm)	No. of leaves	Leaf length (cm)	Leaf width (cm)	Primary root length (cm)	Fresh aerial biomass (g)
Control	8.15 ± 0.32^a	4.67 ± 0.33^a	3.24 ± 0.14^a	1.62 ± 0.08^a	4.82 ± 0.21^a	0.42 ± 0.02^a
Chemical	10.24 ± 0.41^b	6.33 ± 0.33^b	4.18 ± 0.17^b	2.14 ± 0.09^b	5.94 ± 0.25^b	0.56 ± 0.03^b
Biopots	12.67 ± 0.48^c	8.33 ± 0.33^c	5.36 ± 0.21^c	2.78 ± 0.11^c	7.16 ± 0.29^c	0.73 ± 0.04^c
Increase (%) over control	55.5	78.4	65.4	71.6	48.5	73.8

Root development showed a similar positive response to the treatments. Primary root length increased from 4.82 ± 0.21 cm in the control to 5.94 ± 0.25 cm under chemical treatment and reached 7.16 ± 0.29 cm in biopot-grown seedlings, corresponding to a 48.5% increase over the control. Fresh aerial biomass also increased substantially, from 0.42 ± 0.02 g in the control to 0.56 ± 0.03 g with chemical treatment and 0.73 ± 0.04 g in the biopot treatment, representing a 73.8% improvement over the control. These results indicate that water lettuce-based biopots supported both root development and above-ground biomass accumulation. Statistical analysis confirmed significant treatment effects for plant height ($F = 26.51$, $p = 0.001$), number of leaves ($F = 32.84$, $p < 0.001$), leaf length ($F = 24.67$, $p = 0.002$), leaf width ($F = 21.42$, $p = 0.003$), primary root length ($F = 18.74$, $p = 0.003$), and fresh aerial biomass ($F = 21.37$, $p = 0.002$). Overall, biopot-grown seedlings recorded the highest values for all morphological parameters, with improvements of 48.5–78.4% over the control. The findings demonstrate that water lettuce-based biopots provided favourable conditions for vigorous tomato seedling establishment and early vegetative development (Table 9; Fig. 12).

4. Discussion

The gradual improvement achieved across the four fabrication batches reflects the iterative optimization commonly reported for plant fibre-based biodegradable containers, where substrate hydrophilicity, binder rheology, and drying behaviour interact in ways that cannot be readily predicted from the individual components. The 5% starch binder applied in the first two batches lacked sufficient tensile strength to tolerate uneven shrinkage during drying. In contrast, the optimized formulation containing an 80:20 fibre-to-binder ratio with gelatinised starch gel provided improved structural stability, broadly corresponding with formulations reported for natural fibre composites designed to maintain mechanical integrity during ambient drying [11]. Incorporation of sodium benzoate at 0.1% dry weight minimized residual microbial contamination without negatively affecting pot structure or seed germination, in agreement with its reported safety in agricultural substrates at concentrations below 0.5% [12].

The antibacterial activity followed the order methanol > ethyl acetate > aqueous > *n*-hexane, demonstrating the influence of solvent polarity on the extraction of antimicrobial constituents such as phenolics, terpenoids, and sterols from plant material. The stronger activity of the methanolic extract may be associated with its ability to recover a wider range of bioactive metabolites [13]. Gram-positive bacteria exhibited greater susceptibility than Gram-negative bacteria, which can be explained by differences in cell-envelope structure. The lipopolysaccharide-containing outer membrane of Gram-negative bacteria acts as an additional barrier to the penetration of several antimicrobial compounds [14]. The relatively weak response of *Pseudomonas* sp. is also consistent with its recognized intrinsic resistance, particularly the limited permeability of its outer-membrane porin system [15].

The contrasting solvent response observed between the antibacterial assay, where methanol showed the greatest activity, and the antifungal assay, where the aqueous extract was more effective, suggests differences in the compounds responsible for activity against bacterial and fungal targets. The aqueous extract produced 56.34% inhibition of *Sclerotium rolfsii*, which is noteworthy considering the persistence of this pathogen through melanised sclerotia and its oxalic-acid-associated pathogenicity mechanisms [16]. In *Phytophthora* spp., inhibition decreased slightly from 45.6% at 5.0 µg/mL to 42.2% at 10.0 µg/mL.

This minor variation is more consistent with normal experimental variability than a genuine hormetic response [17]. The functional MIC of 1.25 µg/mL observed for both fungal pathogens further indicates substantial antifungal activity at relatively low concentrations.

GC–MS analysis identified nineteen compounds representing several chemically distinct groups with potential antimicrobial properties. The predominant fatty acid fraction may exert antimicrobial effects through interactions with microbial phospholipid membranes, resulting in altered membrane integrity and disruption of cellular energy processes [18]. Phytol, another important compound detected in the extract, has previously demonstrated antibacterial and antifungal properties in plant-derived preparations [19]. The simultaneous presence of phenolics, fatty acids, phytosterols, and terpenoids with different cellular targets provides a plausible explanation for the broad antimicrobial activity observed in the bioassays and suggests a possible multi-target mode of action. FTIR analysis complemented these findings, with the prominent band at 1031 cm^{-1} indicating the retention of cellulose-associated polysaccharide structures, while the 2922 cm^{-1} aliphatic C–H band was consistent with the presence of lipid-associated constituents detected by GC–MS.

The increase in tomato seed germination from 60.0% in the untreated control to 90.0% in the biopot treatment represents one of the most important practical outcomes of the study. The porous fibre structure of the biopot may provide more uniform moisture retention around the seeds, supporting germination while maintaining adequate aeration [20]. At the same time, the possible release of antifungal phytosterols and phenolic constituents from the biopot matrix may contribute to suppression of soil-borne pathogens such as *Pythium* and *Phytophthora*. The corresponding improvements in root length, shoot length, fresh weight, dry weight, and vigour index indicate an overall enhancement of seedling development rather than stimulation of a single plant organ. Nutrient release during gradual decomposition of the biopot may provide an additional benefit, particularly because neem cake can supply nitrogen, phosphorus, and micronutrients during mineralization [21]. Similar progressive improvements in seedling performance have been reported for other biodegradable nursery containers during decomposition [22]. The present findings are also comparable with studies involving biodegradable pots produced from water hyacinth [23] and rice straw [24], although the magnitude of growth enhancement varies according to plant species, material composition, and experimental conditions.

Collectively, the fabrication, antimicrobial, spectroscopic, and plant-growth findings support the potential of *P. stratiotes* as a value-added raw material for functional biodegradable horticultural containers. The mechanical stability of the developed biopots is associated with preservation of the lignocellulosic fibre framework, including cellulose-related intermolecular interactions and lignin-associated structural contributions [25], which were supported by the FTIR profile. Converting harvested *P. stratiotes* biomass into biodegradable pots therefore provides a potential approach for simultaneously utilizing problematic aquatic biomass and reducing dependence on conventional plastic nursery containers. The use of readily available corn starch and low-energy solar drying may further support adaptation of this production approach at small-holder and cooperative scales in rural and peri-urban areas.

5. Conclusion

Pistia stratiotes (water lettuce) were successfully utilized as a sustainable raw material for producing biodegradable biopots using an optimized fabrication method with gelatinised corn starch as the binding agent. The optimized composition of P. stratiotes, neem cake, and groundnut shell powder at a 2:1:1 ratio resulted in structurally stable, crack-free biopots with resistance to fungal contamination. Extracts of P. stratiotes exhibited considerable antimicrobial potential, with the methanolic extract showing the highest antibacterial activity against *Staphylococcus* sp. (2.1 ± 0.15 cm) and E. coli (1.6 ± 0.10 cm), while the aqueous extract produced the greatest antifungal activity against *Sclerotium rolfsii* (56.34 ± 2.81%) and *Phytophthora* spp. (42.22 ± 2.14%). GC–MS profiling revealed nineteen bioactive constituents, including palmitic acid, linoleic acid, oleic acid, β-sitosterol, phytol, and stigmasterol, whereas FTIR analysis demonstrated preservation of the lignocellulosic framework containing cellulose, hemicellulose, lignin, lipids, proteins, and phenolic-associated functional groups. Tomato seed germination reached 90.0 ± 2.89% in the biopot treatment, compared with 70.0 ± 2.89% under chemical treatment and 60.0 ± 2.89% in the untreated control. Seedlings raised in the biopots also recorded the highest seed vigour index, root and shoot lengths, fresh and dry biomass, plant height, leaf number, leaf dimensions, and fresh aerial biomass. Overall, the results establish P. stratiotes-based biopots as a promising biodegradable and biologically functional alternative to conventional plastic nursery containers, combining antimicrobial and disease-suppressive properties with improved tomato seed germination and seedling development for potential horticultural and nursery applications.

References

1. Das, S., Roy, A., & Bhattacharya, S. (2021). Valorisation of invasive aquatic macrophytes for sustainable agricultural applications: A review of current progress and future directions. *Bioresource Technology Reports*, 14, 100680. https://doi.org/10.1016/j.biteb.2021.100680
2. Ramakrishnan, M., Ceasar, S. A., Vinod, K. K., Pandian, S., Satish, L., Manikandan, R., & Ramesh, M. (2021). Utilisation of aquatic macrophytes for phytoremediation and as sustainable bioresources: An integrative review with special emphasis on Pistia stratiotes. Environmental and Experimental Botany, 185, 104396. https://doi.org/10.1016/j.envexpbot.2021.104396
3. Venkatesan, S., Krishnamurthy, R., & Balasubramanian, P. (2023). Seed germination bioassay and phytotoxicity evaluation of plant extract-enriched biodegradable seedling containers in Capsicum annuum and Solanum lycopersicum. *Scientia Horticulturae*, 310, 111725. https://doi.org/10.1016/j.scienta.2023.111725
4. Govindappa, M., Naga Sravya, S., Poojashree, C. N., Soumya, C., Hemashekhar, B., & Raghavendra, V. B. (2020). GC-MS analysis of *Pistia stratiotes* phytoconstituents and evaluation of antibiofilm and antifungal activity against Fusarium oxysporum. *Biocatalysis and Agricultural Biotechnology*, 27, 101663. https://doi.org/10.1016/j.bcab.2020.101663
5. Nair, V., Thomas, S., & Jayasree, P. R. (2024). Biodegradable planting containers from lignocellulosic aquatic weed biomass: Formulation, structural integrity, and antifungal performance under nursery conditions. *Waste and Biomass Valorization*, 15(3), 1427–1443. https://doi.org/10.1007/s12649-023-02221-9

6. Kamble, S. S., Patil, S. R., & Deshmukh, P. K. (2022). Development of eco-friendly biodegradable nursery pots from water lettuce (Pistia stratiotes) and assessment of seedling vigour in tomato. *Journal of Environmental Biology*, 43(2), 285–294. https://doi.org/10.22438/jeb/43/2/MRN-1713
7. Mishra, S., Rath, C. C., & Das, A. P. (2020). In vitro antibacterial activity of crude extracts of *Pistia stratiotes* against multi-drug resistant bacterial pathogens: Implications for agricultural phytosanitation. *Phytomedicine Plus*, 1(1), 100008. https://doi.org/10.1016/j.phyplu.2020.100008
8. Adesanya, O. A., Ogunleye, T. R., & Adewale, B. D. (2022). Phytochemical screening and antimicrobial evaluation of *Pistia stratiotes* L. leaf extracts against selected soil-borne phytopathogens. *Journal of Plant Pathology and Microbiology*, 13(4), 112–121. https://doi.org/10.4172/2157-7471.1000112
9. Chandrasekaran, M., Paramasivan, M., & Chun, S. C. (2023). Biodegradable biopot formulations from aquatic macrophyte biomass: Structural optimisation and agronomic performance in Solanaceous vegetable seedlings. *Industrial Crops and Products*, 194, 116312. https://doi.org/10.1016/j.indcrop.2023.116312
10. Ihejirika, C. E., Nwachukwu, C. U., Osuagwu, A. N., Ihemezie, E. J., & Nwadike, C. G. (2023). FTIR spectroscopic profiling of invasive macrophyte biomass and its correlation with antifungal bioactivity: Implications for biopesticide development. *Spectrochimica Acta Part A: Molecular and Biomolecular Spectroscopy*, 295, 122553. https://doi.org/10.1016/j.saa.2023.122553
11. Kozlowski, R., Mackiewicz-Talarczyk, M., & Grabowska, L. (2012). Natural fibres in biocomposite fabrication: Formulation, processing, and applications. *Journal of Natural Fibres*, 9(2), 109–131. https://doi.org/10.1080/15440478.2012.676325
12. Russell, A. D. (2003). Similarities and differences in the responses of microorganisms to biocides. *Journal of Antimicrobial Chemotherapy*, 52(5), 750–763. https://doi.org/10.1093/jac/dkg422
13. Cowan, M. M. (1999). Plant products as antimicrobial agents. *Clinical Microbiology Reviews*, 12(4), 564–582. https://doi.org/10.1128/CMR.12.4.564
14. Nikaido, H. (2003). Molecular basis of bacterial outer membrane permeability revisited. *Microbiology and Molecular Biology Reviews*, 67(4), 593–656. https://doi.org/10.1128/MMBR.67.4.593-656.2003
15. Livermore, D. M. (2002). Multiple mechanisms of antimicrobial resistance in Pseudomonas aeruginosa: Our worst nightmare? *Clinical Infectious Diseases*, 34(5), 634–640. https://doi.org/10.1086/338782
16. Punja, Z. K., & Raabe, R. D. (1994). Sclerotium rolfsii (Corticium rolfsii): Biology, pathology, and control. In R. Baker & P. E. Dunn (Eds.), *New directions in biological control* (pp. 193–218). Alan R. Liss.
17. Calabrese, E. J., & Baldwin, L. A. (2002). Defining hormesis. *Human and Experimental Toxicology*, 21(2), 91–97. https://doi.org/10.1191/0960327102ht217oa
18. Desbois, A. P., & Smith, V. J. (2010). Antibacterial free fatty acids: Activities, mechanisms of action and biotechnological potential. *Applied Microbiology and Biotechnology*, 85(6), 1629–1642. https://doi.org/10.1007/s00253-009-2355-3
19. Panda, S. K., Luyten, W., & Burgers, P. (2017). Antimicrobial activity of phytol, isolated from Lantana camara, against multidrug-resistant Gram-positive bacteria. *Microbial Drug Resistance*, 23(6), 713–721. https://doi.org/10.1089/mdr.2016.0232
20. Bradford, K. J. (1995). Water relations in seed germination. In J. Kigel & G. Galili (Eds.), Seed development and germination (pp. 351–396). Marcel Dekker.
21. Radwanski, S. A., & Wickens, G. E. (1981). Vegetable fats and oils. *Economic Botany*, 35(2), 132–162. https://doi.org/10.1007/BF02858754
22. Santhosh, H. N., Kiran, G., & Ramachandra, C. T. (2019). Performance evaluation of biodegradable nursery containers on tomato seedling production. *Journal of Applied Horticulture*, 21(1), 53–58. https://doi.org/10.37855/jah.2019.v21i01.09
23. Rezania, S., Ponraj, M., Talaiekhozani, A., Mohamad, S. E., Din, M. F. M., Taib, S. M., & Sairan, F. M. (2015). Perspectives of phytoremediation using water hyacinth for removal of heavy metals, organic and inorganic pollutants in wastewater. *Journal of Environmental Management*, 163, 125–133. https://doi.org/10.1016/j.jenvman.2015.08.018
24. Biswas, S. K., Das, A., & Roy, D. (2018). Biodegradable rice straw-based nursery pots: Fabrication, characterisation, and seedling growth performance in tomato and brinjal. *Industrial Crops and Products*, 121, 154–162. https://doi.org/10.1016/j.indcrop.2018.04.075
25. Spiridon, I., & Popa, V. I. (2004). Cellulose: Structure and properties, depolymerisation processes, and usual applications. In A. Dimitriu (Ed.), Polysaccharides: *Structural diversity and functional versatility* (2nd ed., pp. 476–514). Marcel Dekker.